



<b>Title</b>	Single-nucleotide polymorphisms in human NPC1 influence filovirus entry into cells
<b>Author(s)</b>	Kondoh, Tatsunari; Letko, Michael; Munster, Vincent J.; Manzoor, Rashid; Maruyama, Junki; Furuyama, Wakako; Miyamoto, Hiroko; Shigeno, Asako; Fujikura, Daisuke; Takadate, Yoshihiro; Yoshida, Reiko; Igarashi, Manabu; Feldmann, Heinz; Marzi, Andrea; Takada, Ayato
<b>Citation</b>	Journal of Infectious Diseases, 218(suppl 5), S397-S402 <a href="https://doi.org/10.1093/infdis/jiy248">https://doi.org/10.1093/infdis/jiy248</a>
<b>Issue Date</b>	2018-12-15
<b>Doc URL</b>	<a href="http://hdl.handle.net/2115/76336">http://hdl.handle.net/2115/76336</a>
<b>Rights</b>	This is a pre-copyedited, author-produced version of an article accepted for publication in The Journal of Infectious Diseases following peer review. The version of record Volume 218 Issue suppl_5, S397-S402, 2018 is available online at: <a href="https://doi.org/10.1093/infdis/jiy248">https://doi.org/10.1093/infdis/jiy248</a> .
<b>Type</b>	article (author version)
<b>File Information</b>	JID-64220_R1.pdf



[Instructions for use](#)

1 **Single nucleotide polymorphisms in human NPC1 influence filovirus entry into cells**

2

3 Tatsunari Kondoh,<sup>1</sup> Michael Letko,<sup>2</sup> Vincent J. Munster,<sup>2</sup> Rashid Manzoor,<sup>1</sup> Junki  
4 Maruyama,<sup>1,a</sup> Wakako Furuyama,<sup>1,b</sup> Hiroko Miyamoto,<sup>1</sup> Asako Shigeno,<sup>1</sup> Daisuke  
5 Fujikura,<sup>3,c</sup> Yoshihiro Takadate,<sup>1</sup> Reiko Yoshida,<sup>1</sup> Manabu Igarashi,<sup>1,4</sup> Heinz Feldmann,<sup>2</sup>  
6 Andrea Marzi,<sup>2</sup> and Ayato Takada<sup>1,4,5\*</sup>

7

8 <sup>1</sup>Division of Global Epidemiology, Research Center for Zoonosis Control, Hokkaido  
9 University, Sapporo, Japan; <sup>2</sup>Laboratory of Virology, Division of Intramural Research,  
10 National Institute of Allergy and Infectious Diseases, National Institutes of Health, Rocky  
11 Mountain Laboratories, Hamilton, Montana, USA; <sup>3</sup>Division of Infection and Immunity,  
12 Research Center for Zoonosis Control, Hokkaido University, Sapporo, Japan; <sup>4</sup>Global  
13 Station for Zoonosis Control, Global Institution for Collaborative Research and  
14 Education, Hokkaido University, Sapporo, Japan; <sup>5</sup>School of Veterinary Medicine, the  
15 University of Zambia, Lusaka, Zambia

16

17 **Running title**

18 Human NPC1 SNPs influence filovirus infection

19

20 The character and space count of the title: 82

21 The character and space count of the running title: 45

22 The word count of the abstract: 150

23 The word count of the main text: 2057

24

25 **Footnote**

26

27 **Conflict of Interest:** We have no potential conflicts of interest in relation to this research.

28

29 **Financial support:** This work was supported by a Research Fellowship for Young  
30 Scientists from the Japan Society for the Promotion of Science (JSPS)(16J04404) and  
31 KAKENHI (16H02627 and 15H01249) from JSPS and the Ministry of Education, Culture,  
32 Sports, Science and Technology (MEXT) of Japan. Funding was also provided in part by  
33 the Intramural Research Program, NIAID, NIH and by the Japanese Initiative for Progress  
34 of Research on Infectious Disease for Global Epidemics (J-PRIDE)(JP17fm0208101)  
35 from the Japan Agency for Medical Research and Development (AMED).

36

37 **Correspondence:** Ayato Takada, DVM, PhD, Division of Global Epidemiology,  
38 Research Center for Zoonosis Control, Hokkaido University, Kita-20, Nishi-10, Kita-ku,  
39 Sapporo 001-0020, Japan (atakada@czc.hokudai.ac.jp), TEL: +81-11-706-9502, FAX:  
40 +81-11-706-7310.

41

42 **Present address**

43 <sup>a</sup>Department of Pathology, The University of Texas Medical Branch, Galveston, Texas,  
44 USA (Junki Maruyama); <sup>b</sup>Laboratory of Virology, Division of Intramural Research,  
45 National Institute of Allergy and Infectious Diseases, National Institutes of Health,  
46 Rocky Mountain Laboratories, Hamilton, Montana, USA (Wakako Furuyama); <sup>c</sup>Center  
47 for Advanced Research and Education (CARE), Asahikawa Medical University,  
48 Asahikawa, Japan (Daisuke Fujikura)

49

50 **ABSTRACT**

51 Niemann-Pick C1 (NPC1), a host receptor involved in the envelope glycoprotein  
52 (GP)-mediated entry of filoviruses into cells, is believed to be a major determinant of cell  
53 susceptibility to filovirus infection. It is known that proteolytically digested Ebola virus  
54 (EBOV) GP interacts with two protruding loops in domain C of NPC1. Using previously  
55 published structural data and the single nucleotide polymorphisms (SNPs) database, we  
56 identified ten naturally occurring, missense SNPs in human NPC1. To investigate whether  
57 these SNPs affect cell susceptibility to filovirus infection, we generated Vero E6 cell lines  
58 stably expressing NPC1 with SNP substitutions and compared their susceptibility to  
59 vesicular stomatitis virus pseudotyped with filovirus GPs and infectious EBOV. We found  
60 that some of the substitutions resulted in reduced susceptibility to filoviruses as indicated  
61 by the lower titers and smaller plaque/focus sizes of the viruses. Our data suggest that  
62 human NPC1 SNPs may likely affect host susceptibility to filoviruses.

63

64 Key words: Ebolavirus, Marburgvirus, Niemann-Pick C1 (NPC1), single nucleotide  
65 polymorphism (SNP), NPC1 knockout Vero E6 (Vero E6/NPC1-KO)

66

67 **INTRODUCTION**

68           Ebolaviruses and marburgviruses are members of the family *Filoviridae* and  
69 cause severe hemorrhagic fever in humans and nonhuman primates. *Filoviridae* consists  
70 of three genera, encompassing seven species (5, 1, and 1 species in the genera *Ebolavirus*,  
71 *Marburgvirus*, and *Cuevavirus*, respectively) [1]. Currently, eight distinct viruses are  
72 assigned to these seven species: Ebola virus (EBOV), Bundibugyo virus (BDBV), Tai  
73 Forest virus (TAFV), Sudan virus (SUDV), and Reston virus (RESTV) in the genus  
74 *Ebolavirus*; Marburg virus (MARV) and Ravn virus (RAVV) in the genus *Marburgvirus*;  
75 and Lloviu virus (LLOV) in the genus *Cuevavirus*. The biological properties of LLOV  
76 are uncharacterized since infectious LLOV has not been isolated yet. Filoviruses have  
77 continuously produced sporadic outbreaks with increased frequency in Central and West  
78 Africa and are considered a significant public health concern.

79           The envelope glycoprotein (GP) is the only viral surface protein of filoviruses  
80 and mediates viral entry into cells [2]. After binding to attachment factors such as C-type  
81 lectins [3, 4], virus particles are internalized into host cells via macropinocytosis [5-7].  
82 Late endosomal low pH leads to cysteine protease-mediated proteolysis of the viral GP  
83 [8, 9]. This digested GP (dGP) can then interact with the host endosomal fusion receptor,  
84 Niemann-Pick C1 (NPC1), allowing fusion between the viral envelope and the host  
85 endosomal membrane [10-12]. Thus, NPC1 represents a major determinant of cell  
86 susceptibility to filovirus infection [13, 14].

87           The recently published co-structures of EBOV dGP in complex with NPC1  
88 revealed that two surface-exposed loops on NPC1 mediate the interaction with dGP [15,  
89 16]. Biochemical analysis of purified NPC1 and dGP has further shown that amino acid  
90 substitutions in these two loops (e.g., P424A, F503G and F504G) reduce the binding to

91 dGP [15]. This finding led us to hypothesize that single nucleotide polymorphisms (SNPs)  
92 in human NPC1 might influence host susceptibility to filovirus infection. Mutations tested  
93 in previous studies [13-15] were not linked to human NPC1 SNPs and are unregistered in  
94 the SNP database (<https://www.ncbi.nlm.nih.gov/snp/>); thus it remains unknown whether  
95 naturally occurring SNPs found in human NPC1 can affect the efficiency of filovirus  
96 infection.

97         Using a structural-guided approach to the SNP database, we identified ten  
98 missense SNPs in the GP-interacting loop regions of NPC1. To investigate the potential  
99 effects of these substitutions on filovirus infection in vitro, we generated an NPC1  
100 knockout Vero E6 cell line and established stable cell lines expressing the NPC1 SNP  
101 mutants. Cell susceptibility was examined using vesicular stomatitis virus (VSV)  
102 pseudotyped with filovirus GPs [2, 17] as well as a replication-competent EBOV  
103 expressing green fluorescent protein (GFP) [18]. Here, we report human NPC1 SNPs that  
104 influence the susceptibility of cells to filovirus entry and infection.

105

## 106 **MATERIALS AND METHODS**

### 107 **Viruses**

108         VSV containing the GFP gene instead of the receptor-binding VSV-G protein  
109 gene (VSV $\Delta$ G) and pseudotyped viruses with GPs of EBOV (Mayinga), BDBV (Butalya),  
110 TAFV (Pauléoula), SUDV (Boniface), RESTV (Pennsylvania), MARV (Angola), RAVV  
111 (Kitum Cave), and LLOV (Asturias), designated by VSV $\Delta$ G-EBOV, -BDBV, -TAFV, -  
112 SUDV, - RESTV, - MARV, - RAVV, and - LLOV, respectively, were generated as  
113 described previously [2, 19]. Infectious units (IUs) of these pseudotyped VSVs were  
114 determined in Vero E6 cells as previously described [2, 20]. Replication-competent

115 recombinant VSVs (rVSV-EBOV [Mayinga] and rVSV-MARV [Angola]) were generated  
116 as described previously [17]. rVSV-EBOV, rVSV-MARV, and recombinant EBOV  
117 expressing GFP (EBOV-GFP) [18] were propagated in Vero E6 cells and stored at -80°C.  
118 Infectivity of rVSV-EBOV, rVSV-MARV, and EBOV-GFP in each cell line was  
119 determined by plaque- and focus-forming assays, respectively, as described previously  
120 [21, 22]. Relative infectivity in each cell line was calculated by setting IU, plaque forming  
121 unit, or focus forming unit values given by Vero E6 cells expressing 293T-NPC1 to 100%.

122

### 123 **Biosafety**

124 All infectious work with EBOV-GFP was performed in the biosafety level-4  
125 laboratory (BSL-4) at the Integrated Research Facility of the Rocky Mountain  
126 Laboratories, Division of Intramural Research, National Institute of Allergy and  
127 Infectious Diseases, National Institutes of Health, Hamilton, Montana, USA. All Standard  
128 Operating Procedures (SOPs) were approved by the Institutional Biosafety Committee  
129 (IBC)

130

### 131 **Cell lines**

132 Vero E6, NPC1 knockout Vero E6 (Vero E6/NPC1-KO) and HEK293T-derived  
133 Platinum-GP (Plat-GP) cells [23] (Cell Biolabs) were grown in Dulbecco's modified  
134 Eagle's medium (DMEM, Sigma-Aldrich) supplemented with 10% fetal calf serum. Vero  
135 E6/NPC1-KO cells were generated by previously described methods [24, 25] with a few  
136 modifications and transduced with retroviruses expressing HEK293T-derived NPC1 and  
137 its mutant genes (see Supplementary Materials and Methods).

138

139 **Cloning of the NPC1 gene into plasmids**

140 The coding region of the HEK293T NPC1 gene was polymerase chain reaction  
141 (PCR)-amplified from cDNA prepared from total RNA extracted from HEK293T cells  
142 according to a previous study [26]. The PCR product was cloned into a murine leukemia  
143 virus-based retroviral vector, pMXs-puro [23]. Ten SNPs found in the two loops:  
144 rs772847092 (I419V and I419F), rs77815278 (Y420S), rs771644708 (Y420H),  
145 rs143797098 (P424A), rs140149624 (S425L), rs749078710 (A427T), rs748246747  
146 (G500E), rs191537721 (D502E), and rs756587493 (D508N), were produced by site-  
147 directed mutagenesis using a KOD-Plus-Neo polymerase (TOYOBO) with primers  
148 containing the desired nucleotide substitutions. All mutations were confirmed by DNA  
149 sequencing.

150

151 **Statistical analysis**

152 All statistical analyses were performed using R software (version 3.2.3) [27].  
153 Correlations between transcription and expression levels of NPC1 were estimated using  
154 the rank correlation coefficient of Spearman ( $r_s$ ). For comparison of viral infectivity and  
155 plaque/focus size, the one-way ANOVA followed by Dunnett's tests and Welch's t-test  
156 were used. *P*-values of less than 0.05 were considered to be statistically significant.

157

158



159 **RESULTS**

160 **Structure-guided approach to identifying candidate NPC1 SNPs**

161 Human NPC1 has at least 254 unique SNPs listed in the SNP database  
162 (<https://www.ncbi.nlm.nih.gov/snp/>). Of these SNPs, 222 are missense, resulting in amino  
163 acid changes, and they are widely distributed throughout the structure of NPC1 (Figure  
164 1A). Using the co-structure of full-length NPC1 and EBOV dGP [16], we identified 10  
165 missense SNPs in 8 amino acid positions located in the interface (i.e., 2 loop structures at  
166 amino acid positions 419-428 and 500-508) with EBOV GP (Figure 1B).

167

168 **Human NPC1 polymorphisms affecting filovirus entry into cells**

169 We next established an NPC1 knockout Vero E6 cell line, Vero E6/NPC1-KO  
170 cl.19 (Supplementary Figure 1A and B), and confirmed that its susceptibility to VSV $\Delta$ G-  
171 EBOV, rVSV-EBOV, and EBOV-GFP was completely abolished (Supplementary Figure  
172 1C-E). The Vero E6/NPC1-KO cl.19 cells were then transduced with a retroviral vector  
173 resulting in eleven different cell lines stably expressing wild-type human NPC1 (293T-  
174 NPC1) or NPC1 SNP mutants (I419V, I419F, Y420S, Y420H, P424A, S425L, A427T,  
175 G500E, D502E, and D508N). Introducing the wild-type NPC1 gene into the knockout  
176 cells completely restored the susceptibility to filovirus entry and infection  
177 (Supplementary Figure 1C-E), as has been shown with NPC1-deficient CHO and reptile-  
178 derived cells [10, 12]. Transcription and expression levels of the transduced NPC1 genes  
179 were examined by quantitative PCR and western blot analyses, respectively (see  
180 Supplementary Materials and Methods). In all of the NPC1 SNP mutant cell lines,  
181 expression levels of NPC1 were equivalent to or higher than those of 293T-NPC1-  
182 expressing cells (Supplementary Figure 2). We also confirmed that these NPC1s were

183 similarly localized at endosomal vesicles (data not shown).

184 To evaluate whether these SNP substitutions affected the efficiency of viral entry,  
185 each cell line was infected with replication-incompetent VSV pseudotyped with filovirus  
186 GPs, and relative IUs were compared among the cell lines (Figure 2). We found that  
187 P424A, S425L, D502E, and D508N substitutions in NPC1 reduced the entry of VSV  
188 pseudotyped with GPs from multiple filovirus species. P424A and D508N substitutions  
189 significantly affected the entry of VSVΔG- EBOV, - BDBV, - TAFV, - SUDV, - RESTV,  
190 and - LLOV, but not MARV and/or -RAVV. On the other hand, S425L and D502E  
191 substitutions reduced the entry of VSVΔG-MARV, and some of the pseudotyped VSV  
192 with ebolavirus GPs. Y420S substitution only reduced the entry of VSVΔG-LLOV. It was  
193 noted that these substitutions resulted in different patterns of reduction corresponding to  
194 the filovirus genera (i.e., *Ebolavirus*, *Marburgvirus*, and *Cuevavirus*). In particular,  
195 P424A/D508N and S425L/D502E substitutions seemed to be important for the reduced  
196 entry of VSVs pseudotyped with ebolavirus and marburgvirus GPs, respectively. In some  
197 cell lines, infectivity of the viruses was enhanced and it was correlated with relatively  
198 high expression levels of NPC1 (Supplementary Figure 2).

199

#### 200 **Reduced plaque-forming ability of rVSV-EBOV in Vero E6 cells expressing NPC1** 201 **with P424A or D508N substitution**

202 We then compared the plaque-forming abilities of rVSV-EBOV and rVSV-  
203 MARV using the same cell lines (Figure 3). Although statistically significant difference  
204 was not observed, the P424A and S425L substitutions moderately reduced the plaque  
205 number of rVSV-EBOV and rVSV-MARV, respectively (Figure 3A). As expected, the  
206 average plaque sizes of rVSV-EBOV in cells expressing NPC1 with the D508N

207 substitution were significantly smaller than in 293T-NPC1-expressing cells and the  
208 P424A substitution also slightly reduced the plaque size (Figure 3B). Consistent with the  
209 data shown in Figure 2, rVSV-MARV formed slightly, but not significantly, smaller  
210 plaques in the cell line expressing S425L NPC1 (Figure 3B).

211

### 212 **Reduced focus-forming ability of EBOV in Vero E6 cells with the P424A substitution**

213 To examine the effects of substitutions associated with NPC1 SNPs on actual  
214 filovirus infection, we used an infectious EBOV expressing GFP and determined the viral  
215 focus numbers and average focus size in each cell line. Consistent with our pseudotyped  
216 VSV data, the P424A substitution resulted in reduced focus numbers of EBOV-GFP  
217 (Figure 3C). The average size of foci in this cell line was also smaller than in cells  
218 expressing 293T-NPC1 (Figure 3D). Although these differences were not significant in a  
219 multiple comparison analysis, Welch's t-test gave significant differences compared to  
220 293T-NPC1-expressing cells. The D508N substitution slightly reduced the focus size of  
221 EBOV-GFP but there was no statistically significant difference compared to 293T-NPC1-  
222 expressing cells.

223

224

225 **DISCUSSION**

226 With human immunodeficiency virus type 1 (HIV-1) infection, there is a subset  
227 of people who are inherently resistant to the virus [28-31]. In particular, genetic variation  
228 in the host viral receptors has been shown to reduce the susceptibility to HIV infection in  
229 humans [28, 29]. Though asymptomatic filovirus infection is less studied, Baron et al.  
230 [32] reported potential asymptomatic cases during the outbreak in Sudan in 1979, and  
231 Dean et al. [33] estimated the proportion of asymptomatic transmissions during the recent  
232 epidemic in West Africa. Although host genetics and Ebola virus disease progression and  
233 resistance have been studied in mice [34, 35], the details of genetic polymorphisms that  
234 may affect susceptibility of humans to filoviruses have not been elucidated yet.

235 In the present study, we focused on ten reported NPC1 SNP substitutions that  
236 interface with GP. Although none of the SNPs tested here completely ablated viral entry  
237 or infectivity, some SNPs were nevertheless found to be important for filovirus infection.  
238 In our experiments, P424A substitution reduced entry of VSV pseudotyped with  
239 ebolavirus but not marburgvirus GPs. Moreover, focus sizes of EBOV-GFP were also  
240 reduced in this cell line. Interestingly, Wang et al. [15] demonstrated that the P424A NPC1  
241 mutant retained binding capacity to dGP but with reduced affinity compared to wild-type  
242 NPC1. Taken together, these findings suggest that the P424A substitution in NPC1 lowers  
243 its binding capacity to dGP, resulting in reduced viral entry and infection.

244 S425L substitution also reduced the infection with some pseudotyped VSVs,  
245 including VSV $\Delta$ G-MARV and -RAVV. The serine residue at position 425 in NPC1 was  
246 shown to be involved in the interaction with the amino acid residue at position 142 of the  
247 EBOV GP molecule [15]. However, since amino acid residues at this position are different  
248 in EBOV and MARV GPs (serine at 142 of EBOV GP and glutamine at 126 of MARV

249 GP, respectively), the effects of S425L substitution might be different between EBOV and  
250 MARV. It has also been demonstrated that single amino acid mutations at positions 502  
251 or 503 in NPC1 can reduce viral infection [13, 14]. Our experiments confirmed this  
252 finding as D502E substitution reduced the entry of some of the pseudotyped viruses we  
253 tested and also reduced infection with EBOV-GFP (although not significantly). Notably,  
254 while the previous study introduced a significant loss of charge at residue 502 by mutating  
255 the aspartic acid to phenylalanine [13], our study shows that even minimal variation at  
256 this residue (D to E) can have an effect on viral entry.

257         Some other amino acids that are also important for binding to dGP have not been  
258 reported as SNP sites in the NPC1 loops [15]. The rapidly increasing sequence data in  
259 public databases may hereafter provide additional information on NPC1 SNP  
260 substitutions not evaluated in this study. It is also of interest to investigate multiple SNP  
261 substituins in the loops. Although more sensitive studies are needed to further assess the  
262 capacity for NPC1 variation to influence filovirus infection, identifying genetic variations  
263 that affect the susceptibility of hosts to filoviruses will be crucial in understanding  
264 filovirus disease progression and host cell-restriction.

265

266

267 **Supplementary Data**

268 Supplementary materials are available at The Journal of Infectious Diseases online.  
269 Consisting of data provided by the authors to benefit the reader, the posted materials are  
270 not copyedited and are the sole responsibility of the authors, so questions or comments  
271 should be addressed to the corresponding author.

272

273 **Notes**

274 *Acknowledgments.* The authors would like to thank GE Healthcare Japan Corporation  
275 and Koshin Kagaku K.K. for their assistance in the establishment of the IN Cell Analyzer  
276 2000 protocol, Life Technologies Japan, Ltd. and Frontier Science co., Ltd. for their  
277 assistance in gene editing, and Kim Barrymore for editing the manuscript. The authors  
278 would also like to thank Michihito Sasaki (Division of Molecular Pathobiology, Research  
279 Center for Zoonosis Control, Hokkaido University) for anti-LAMP1 antibody.

280

281 **References**

- 282 1. Kuhn JH. Guide to the correct use of filoviral nomenclature. *Curr Top Microbiol*  
283 *Immunol* **2017**; 411:447-460.
- 284 2. Takada A, Robison C, Goto H, et al. A system for functional analysis of Ebola virus  
285 glycoprotein. *Proceedings of the National Academy of Sciences of the United States*  
286 *of America* **1997**; 94:14764-9.
- 287 3. Hofmann-Winkler H, Kaup F, Pöhlmann S. Host cell factors in filovirus entry: Novel  
288 players, new insights. *Viruses* **2012**; 4:3336-62.
- 289 4. Takada A. Filovirus tropism: cellular molecules for viral entry. *Front Microbiol* **2012**;  
290 3:34.
- 291 5. Nanbo A, Imai M, Watanabe S, et al. Ebolavirus is internalized into host cells via  
292 macropinocytosis in a viral glycoprotein-dependent manner. *PLoS Pathog* **2010**;  
293 6:e1001121.
- 294 6. Saeed MF, Kolokoltsov AA, Albrecht T, Davey RA. Cellular entry of Ebola virus  
295 involves uptake by a macropinocytosis-like mechanism and subsequent trafficking  
296 through early and late endosomes. *PLoS Pathog* **2010**; 6:e1001110.
- 297 7. Aleksandrowicz P, Marzi A, Biedenkopf N, et al. Ebola virus enters host cells by  
298 macropinocytosis and clathrin-mediated endocytosis. *J Infect Dis* **2011**; 204 Suppl  
299 3:S957-67.
- 300 8. Chandran K, Sullivan NJ, Felbor U, Whelan SP, Cunningham JM. Endosomal  
301 proteolysis of the Ebola virus glycoprotein is necessary for infection. *Science* **2005**;  
302 308:1643-5.
- 303 9. Misasi J, Chandran K, Yang J-Y, et al. Filoviruses require endosomal cysteine  
304 proteases for entry but exhibit distinct protease preferences. *J Virol* **2012**; 86:3284-

- 305 92.
- 306 10. Carette JE, Raaben M, Wong AC, et al. Ebola virus entry requires the cholesterol  
307 transporter Niemann-Pick C1. *Nature* **2011**; 477:340-3.
- 308 11. Cote M, Misasi J, Ren T, et al. Small molecule inhibitors reveal Niemann-Pick C1 is  
309 essential for Ebola virus infection. *Nature* **2011**; 477:344-8.
- 310 12. Miller EH, Obernosterer G, Raaben M, et al. Ebola virus entry requires the host-  
311 programmed recognition of an intracellular receptor. *EMBO J* **2012**; 31:1947-60.
- 312 13. Ng M, Ndungo E, Kaczmarek ME, et al. Filovirus receptor NPC1 contributes to  
313 species-specific patterns of ebolavirus susceptibility in bats. *eLife* **2015**;4:e11785.
- 314 14. Ndungo E, Herbert AS, Raaben M, et al. A single residue in Ebola virus receptor  
315 NPC1 influences cellular host range in reptiles. *mSphere* **2016**; 1: e00007-16.
- 316 15. Wang H, Shi Y, Song J, et al. Ebola viral glycoprotein bound to its endosomal  
317 receptor Niemann-Pick C1. *Cell* **2016**; 164:258-68.
- 318 16. Gong X, Qian HW, Zhou XH, et al. Structural insights into the Niemann-Pick C1  
319 (NPC1)-mediated cholesterol transfer and Ebola infection. *Cell* **2016**; 165:1467-78.
- 320 17. Takada A, Feldmann H, Stroeher U, et al. Identification of protective epitopes on  
321 Ebola virus glycoprotein at the single amino acid level by using recombinant  
322 vesicular stomatitis viruses. *J Virol* **2003**; 77:1069-74.
- 323 18. Ebihara H, Theriault S, Neumann G, et al. In vitro and in vivo characterization of  
324 recombinant Ebola viruses expressing enhanced green fluorescent protein. *J Infect*  
325 *Dis* **2007**; 196 Suppl 2:S313-22.
- 326 19. Furuyama W, Miyamoto H, Yoshida R, Takada A. Quantification of filovirus  
327 glycoprotein-specific antibodies. *Methods Mol Biol (Clifton, NJ)* **2017**; 1628:309-  
328 20.



- 329 20. Maruyama J, Miyamoto H, Kajihara M, et al. Characterization of the envelope  
330 glycoprotein of a novel filovirus, Lloviu virus. *J Virol* **2014**; 88:99-109.
- 331 21. Kajihara M, Nakayama E, Marzi A, Igarashi M, Feldmann H, Takada A. Novel  
332 mutations in Marburg virus glycoprotein associated with viral evasion from antibody  
333 mediated immune pressure. *J Gen Virol* **2013**; 94:876-83.
- 334 22. Ebihara H, Yoshimatsu K, Ogino M, et al. Pathogenicity of Hantaan virus in newborn  
335 mice: genetic reassortant study demonstrating that a single amino acid change in  
336 glycoprotein G1 is related to virulence. *J Virol* **2000**; 74:9245-55.
- 337 23. Kitamura T, Koshino Y, Shibata F, et al. Retrovirus-mediated gene transfer and  
338 expression cloning: Powerful tools in functional genomics. *Exp Hematol* **2003**;  
339 31:1007-14.
- 340 24. Liang XQ, Potter J, Kumar S, et al. Rapid and highly efficient mammalian cell  
341 engineering via Cas9 protein transfection. *J Biotechnol* **2015**; 208:44-53.
- 342 25. Yu X, Liang XQ, Xie HM, et al. Improved delivery of Cas9 protein/gRNA complexes  
343 using lipofectamine CRISPRMAX. *Biotechnol Lett.* **2016**; 38:919-29.
- 344 26. Kuroda M, Fujikura D, Nanbo A, et al. Interaction between TIM-1 and NPC1 is  
345 important for the cellular entry of Ebola virus. *J Virol* **2015**; 89:6481-93.
- 346 27. Team RC. R: A Language and environment for statistical computing. R foundation  
347 for statistical computing, Vienna, Austria **2015**; URL <https://www.R-project.org/>
- 348 28. Liu R, Paxton WA, Choe S, et al. Homozygous defect in HIV-1 coreceptor accounts  
349 for resistance of some multiply-exposed individuals to HIV-1 infection. *Cell* **1996**;  
350 86:367-77.
- 351 29. Samson M, Libert F, Doranz BJ, et al. Resistance to HIV-1 infection in Caucasian  
352 individuals bearing mutant alleles of the CCR-5 chemokine receptor gene. *Nature*

- 353       **1996**; 382:722-5.
- 354   30. O'Brien SJ, Moore JP. The effect of genetic variation in chemokines and their  
355       receptors on HIV transmission and progression to AIDS. *Immunol Rev* **2000**; 177:99-  
356       111.
- 357   31. Pereyra F, Addo MM, Kaufmann DE, et al. Genetic and immunologic heterogeneity  
358       among persons who control HIV infection in the absence of therapy. *J Infect Dis*  
359       **2008**; 197:563-71.
- 360   32. Baron RC, McCormick JB, Zubeir OA. Ebola virus disease in southern Sudan:  
361       hospital dissemination and intrafamilial spread. *Bull World Health Organ* **1983**;  
362       61:997-1003.
- 363   33. Dean NE, Halloran ME, Yang Y, Longini IM. The transmissibility and pathogenicity  
364       of Ebola virus: a systematic review and meta-analysis of household secondary attack  
365       rate and asymptomatic infection. *Clin Infect Dis* **2016**; 62:1277-1286.
- 366   34. Rasmussen AL, Okumura A, Ferris MT, et al. Host genetic diversity enables Ebola  
367       hemorrhagic fever pathogenesis and resistance. *Science* **2014**; 346:987-91.
- 368   35. Hill-Batorski L, Halfmann P, Marzi A, et al. Loss of interleukin 1 receptor antagonist  
369       enhances susceptibility to Ebola virus infection. *J Infect Dis* **2015**; 212 Suppl 2:S329-  
370       35.
- 371
- 372

373 **Figure Legends**

374

375 **Figure 1. Structural-guided approach to human NPC1 SNP selection.**

376 A, 222 missense SNPs are represented in black on the structure from NPC1. B, Co-  
377 structure of EBOV GP (blue) and NPC1 (tan) with amino acid positions of SNPs indicated  
378 in red (PDB: 5JNX) [16].

379

380 **Figure 2. Infectivities of VSV pseudotyped with filovirus GPs in Vero E6 cell lines.**

381 Confluent monolayers of each cell line grown in 96-well plates were infected with  
382 VSV $\Delta$ G-EBOV, VSV $\Delta$ G-BDBV, VSV $\Delta$ G-TAFV, VSV $\Delta$ G-SUDV, VSV $\Delta$ G-RESTV,  
383 VSV $\Delta$ G-MARV, VSV $\Delta$ G-RAVV, and VSV $\Delta$ G-LLOV. Twenty hours later, the virus  
384 infectious unit (IU) in each cell line was determined by counting the number of GFP-  
385 expressing cells with an IN Cell Analyzer 2000 (GE Healthcare). Relative infectivity in  
386 each cell line was calculated by setting the IU value given by Vero E6 cells expressing  
387 293T-NPC1 (approximately 1000-3000 IU/well for each assay) to 100%. Means and  
388 standard errors of thirty replicates are shown. Values significantly lower than for 293T-  
389 NPC1 are indicated (\* $P < 0.05$ , \*\* $P < 0.01$ , \*\*\* $P < 0.001$ ).

390

391 **Figure 3. Plaque/focus formation of rVSV-EBOV, rVSV-MARV, and EBOV-GFP in**  
392 **Vero E6 cell lines**

393 A, rVSV-EBOV and rVSV-MARV (multiplicity of infection = 0.0005 in Vero E6 cells)  
394 were inoculated into Vero E6 cells grown in 6-well tissue culture plates. After adsorption  
395 for 1 hour, the inoculum was removed and the cells were overlaid with Eagle's minimal  
396 essential medium containing 1.0% Bacto Agar (BD) and then incubated for 3 days at

397 37°C. Cells were stained with 0.5 % crystal violet in 10% formalin and the plaque-  
398 forming unit (PFU) in each cell line was determined by counting the number of all visible  
399 plaques per well (i.e., 50-100 plaques for each assay). Data represent means and standard  
400 errors of at least three independent experiments. *B*, Plaque sizes were measured with  
401 Image-J software. Means and standard errors of 50-100 plaques per well are shown. *C*,  
402 EBOV-GFP (multiplicity of infection = 0.002 in Vero E6 cells) were inoculated into  
403 confluent monolayers of Vero E6 cells grown in 96-well tissue culture plates. After  
404 adsorption for 1 hour, the inoculum was replaced with Eagle's minimal essential medium  
405 containing 1.2% carboxymethyl cellulose. After incubation for 3 days at 37°C, the cells  
406 were fixed and GFP foci in each cell line were counted under a fluorescence microscope.  
407 Data represent means and standard errors of triplicate assays. *D*, Focus sizes were  
408 measured with Image-J software. Means and standard errors of 60-150 foci per well are  
409 shown. (*A-D*) Values significantly lower than for 293T-NPC1 are indicated (\* $P < 0.05$ ,  
410 \*\* $P < 0.01$ , \*\*\* $P < 0.001$ ).

1 **Single nucleotide polymorphisms in human NPC1 influence filovirus entry into cells**

2

3 Tatsunari Kondoh,<sup>1</sup> Michael Letko,<sup>2</sup> Vincent J. Munster,<sup>2</sup> Rashid Manzoor,<sup>1</sup> Junki  
4 Maruyama,<sup>1,a</sup> Wakako Furuyama,<sup>1,b</sup> Hiroko Miyamoto,<sup>1</sup> Asako Shigeno,<sup>1</sup> Daisuke  
5 Fujikura,<sup>3,c</sup> Yoshihiro Takadate,<sup>1</sup> Reiko Yoshida,<sup>1</sup> Manabu Igarashi,<sup>1,4</sup> Heinz Feldmann,<sup>2</sup>  
6 Andrea Marzi,<sup>2</sup> and Ayato Takada<sup>1,4,5\*</sup>

7

8 <sup>1</sup>Division of Global Epidemiology, Research Center for Zoonosis Control, Hokkaido  
9 University, Sapporo, Japan; <sup>2</sup>Laboratory of Virology, Division of Intramural Research,  
10 National Institute of Allergy and Infectious Diseases, National Institutes of Health, Rocky  
11 Mountain Laboratories, Hamilton, Montana, USA; <sup>3</sup>Division of Infection and Immunity,  
12 Research Center for Zoonosis Control, Hokkaido University, Sapporo, Japan; <sup>4</sup>Global  
13 Station for Zoonosis Control, Global Institution for Collaborative Research and  
14 Education, Hokkaido University, Sapporo, Japan; <sup>5</sup>School of Veterinary Medicine, the  
15 University of Zambia, Lusaka, Zambia

16

17 **Running title**

18 Human NPC1 SNPs influence filovirus infection

19

20 The character and space count of the title: 82

21 The character and space count of the running title: 45

22 The word count of the abstract: 150

23 The word count of the main text: 2057

24

25 **Footnote**

26

27 **Conflict of Interest:** We have no potential conflicts of interest in relation to this research.

28

29 **Financial support:** This work was supported by a Research Fellowship for Young  
30 Scientists from the Japan Society for the Promotion of Science (JSPS)(16J04404) and  
31 KAKENHI (16H02627 and 15H01249) from JSPS and the Ministry of Education, Culture,  
32 Sports, Science and Technology (MEXT) of Japan. Funding was also provided in part by  
33 the Intramural Research Program, NIAID, NIH and by the Japanese Initiative for Progress  
34 of Research on Infectious Disease for Global Epidemics (J-PRIDE)(JP17fm0208101)  
35 from the Japan Agency for Medical Research and Development (AMED).

36

37 **Correspondence:** Ayato Takada, DVM, PhD, Division of Global Epidemiology,  
38 Research Center for Zoonosis Control, Hokkaido University, Kita-20, Nishi-10, Kita-ku,  
39 Sapporo 001-0020, Japan (atakada@czc.hokudai.ac.jp), TEL: +81-11-706-9502, FAX:  
40 +81-11-706-7310.

41

42 **Present address**

43 <sup>a</sup>Department of Pathology, The University of Texas Medical Branch, Galveston, Texas,  
44 USA (Junki Maruyama); <sup>b</sup>Laboratory of Virology, Division of Intramural Research,  
45 National Institute of Allergy and Infectious Diseases, National Institutes of Health,  
46 Rocky Mountain Laboratories, Hamilton, Montana, USA (Wakako Furuyama); <sup>c</sup>Center  
47 for Advanced Research and Education (CARE), Asahikawa Medical University,  
48 Asahikawa, Japan (Daisuke Fujikura)

49

50 **ABSTRACT**

51 Niemann-Pick C1 (NPC1), a host receptor involved in the envelope glycoprotein  
52 (GP)-mediated entry of filoviruses into cells, is believed to be a major determinant of cell  
53 susceptibility to filovirus infection. It is known that proteolytically digested Ebola virus  
54 (EBOV) GP interacts with two protruding loops in domain C of NPC1. Using previously  
55 published structural data and the single nucleotide polymorphisms (SNPs) database, we  
56 identified ten naturally occurring, missense SNPs in human NPC1. To investigate whether  
57 these SNPs affect cell susceptibility to filovirus infection, we generated Vero E6 cell lines  
58 stably expressing NPC1 with SNP substitutions and compared their susceptibility to  
59 vesicular stomatitis virus pseudotyped with filovirus GPs and infectious EBOV. We found  
60 that some of the substitutions resulted in reduced susceptibility to filoviruses as indicated  
61 by the lower titers and smaller plaque/focus sizes of the viruses. Our data suggest that  
62 human NPC1 SNPs may likely affect host susceptibility to filoviruses.

63

64 Key words: Ebolavirus, Marburgvirus, Niemann-Pick C1 (NPC1), single nucleotide  
65 polymorphism (SNP), NPC1 knockout Vero E6 (Vero E6/NPC1-KO)

66

67 **INTRODUCTION**

68           Ebolaviruses and marburgviruses are members of the family *Filoviridae* and  
69 cause severe hemorrhagic fever in humans and nonhuman primates. *Filoviridae* consists  
70 of three genera, encompassing seven species (5, 1, and 1 species in the genera *Ebolavirus*,  
71 *Marburgvirus*, and *Cuevavirus*, respectively) [1]. Currently, eight distinct viruses are  
72 assigned to these seven species: Ebola virus (EBOV), Bundibugyo virus (BDBV), Tai  
73 Forest virus (TAFV), Sudan virus (SUDV), and Reston virus (RESTV) in the genus  
74 *Ebolavirus*; Marburg virus (MARV) and Ravn virus (RAVV) in the genus *Marburgvirus*;  
75 and Lloviu virus (LLOV) in the genus *Cuevavirus*. The biological properties of LLOV  
76 are uncharacterized since infectious LLOV has not been isolated yet. Filoviruses have  
77 continuously produced sporadic outbreaks with increased frequency in Central and West  
78 Africa and are considered a significant public health concern.

79           The envelope glycoprotein (GP) is the only viral surface protein of filoviruses  
80 and mediates viral entry into cells [2]. After binding to attachment factors such as C-type  
81 lectins [3, 4], virus particles are internalized into host cells via macropinocytosis [5-7].  
82 Late endosomal low pH leads to cysteine protease-mediated proteolysis of the viral GP  
83 [8, 9]. This digested GP (dGP) can then interact with the host endosomal fusion receptor,  
84 Niemann-Pick C1 (NPC1), allowing fusion between the viral envelope and the host  
85 endosomal membrane [10-12]. Thus, NPC1 represents a major determinant of cell  
86 susceptibility to filovirus infection [13, 14].

87           The recently published co-structures of EBOV dGP in complex with NPC1  
88 revealed that two surface-exposed loops on NPC1 mediate the interaction with dGP [15,  
89 16]. Biochemical analysis of purified NPC1 and dGP has further shown that amino acid  
90 substitutions in these two loops (e.g., P424A, F503G and F504G) reduce the binding to



91 dGP [15]. This finding led us to hypothesize that single nucleotide polymorphisms (SNPs)  
92 in human NPC1 might influence host susceptibility to filovirus infection. Mutations tested  
93 in previous studies [13-15] were not linked to human NPC1 SNPs and are unregistered in  
94 the SNP database (<https://www.ncbi.nlm.nih.gov/snp/>); thus it remains unknown whether  
95 naturally occurring SNPs found in human NPC1 can affect the efficiency of filovirus  
96 infection.

97         Using a structural-guided approach to the SNP database, we identified ten  
98 missense SNPs in the GP-interacting loop regions of NPC1. To investigate the potential  
99 effects of these substitutions on filovirus infection in vitro, we generated an NPC1  
100 knockout Vero E6 cell line and established stable cell lines expressing the NPC1 SNP  
101 mutants. Cell susceptibility was examined using vesicular stomatitis virus (VSV)  
102 pseudotyped with filovirus GPs [2, 17] as well as a replication-competent EBOV  
103 expressing green fluorescent protein (GFP) [18]. Here, we report human NPC1 SNPs that  
104 influence the susceptibility of cells to filovirus entry and infection.

105

## 106 **MATERIALS AND METHODS**

### 107 **Viruses**

108         VSV containing the GFP gene instead of the receptor-binding VSV-G protein  
109 gene (VSV $\Delta$ G) and pseudotyped viruses with GPs of EBOV (Mayinga), BDBV (Butalya),  
110 TAFV (Pauléoula), SUDV (Boniface), RESTV (Pennsylvania), MARV (Angola), RAVV  
111 (Kitum Cave), and LLOV (Asturias), designated by VSV $\Delta$ G-EBOV, -BDBV, -TAFV, -  
112 SUDV, - RESTV, - MARV, - RAVV, and - LLOV, respectively, were generated as  
113 described previously [2, 19]. Infectious units (IUs) of these pseudotyped VSVs were  
114 determined in Vero E6 cells as previously described [2, 20]. Replication-competent

115 recombinant VSVs (rVSV-EBOV [Mayinga] and rVSV-MARV [Angola]) were generated  
116 as described previously [17]. rVSV-EBOV, rVSV-MARV, and recombinant EBOV  
117 expressing GFP (EBOV-GFP) [18] were propagated in Vero E6 cells and stored at -80°C.  
118 Infectivity of rVSV-EBOV, rVSV-MARV, and EBOV-GFP in each cell line was  
119 determined by plaque- and focus-forming assays, respectively, as described previously  
120 [21, 22]. Relative infectivity in each cell line was calculated by setting IU, plaque forming  
121 unit, or focus forming unit values given by Vero E6 cells expressing 293T-NPC1 to 100%.

122

### 123 **Biosafety**

124 All infectious work with EBOV-GFP was performed in the biosafety level-4  
125 laboratory (BSL-4) at the Integrated Research Facility of the Rocky Mountain  
126 Laboratories, Division of Intramural Research, National Institute of Allergy and  
127 Infectious Diseases, National Institutes of Health, Hamilton, Montana, USA. All Standard  
128 Operating Procedures (SOPs) were approved by the Institutional Biosafety Committee  
129 (IBC)

130

### 131 **Cell lines**

132 Vero E6, NPC1 knockout Vero E6 (Vero E6/NPC1-KO) and HEK293T-derived  
133 Platinum-GP (Plat-GP) cells [23] (Cell Biolabs) were grown in Dulbecco's modified  
134 Eagle's medium (DMEM, Sigma-Aldrich) supplemented with 10% fetal calf serum. Vero  
135 E6/NPC1-KO cells were generated by previously described methods [24, 25] with a few  
136 modifications and transduced with retroviruses expressing HEK293T-derived NPC1 and  
137 its mutant genes (see Supplementary Materials and Methods).

138

139 **Cloning of the NPC1 gene into plasmids**

140 The coding region of the HEK293T NPC1 gene was polymerase chain reaction  
141 (PCR)-amplified from cDNA prepared from total RNA extracted from HEK293T cells  
142 according to a previous study [26]. The PCR product was cloned into a murine leukemia  
143 virus-based retroviral vector, pMXs-puro [23]. Ten SNPs found in the two loops:  
144 rs772847092 (I419V and I419F), rs77815278 (Y420S), rs771644708 (Y420H),  
145 rs143797098 (P424A), rs140149624 (S425L), rs749078710 (A427T), rs748246747  
146 (G500E), rs191537721 (D502E), and rs756587493 (D508N), were produced by site-  
147 directed mutagenesis using a KOD-Plus-Neo polymerase (TOYOBO) with primers  
148 containing the desired nucleotide substitutions. All mutations were confirmed by DNA  
149 sequencing.

150

151 **Statistical analysis**

152 All statistical analyses were performed using R software (version 3.2.3) [27].  
153 Correlations between transcription and expression levels of NPC1 were estimated using  
154 the rank correlation coefficient of Spearman ( $r_s$ ). For comparison of viral infectivity and  
155 plaque/focus size, the one-way ANOVA followed by Dunnett's tests and Welch's t-test  
156 were used. *P*-values of less than 0.05 were considered to be statistically significant.

157

158

159

160 **RESULTS**

161 **Structure-guided approach to identifying candidate NPC1 SNPs**

162 Human NPC1 has at least 254 unique SNPs listed in the SNP database  
163 (<https://www.ncbi.nlm.nih.gov/snp/>). Of these SNPs, 222 are missense, resulting in amino  
164 acid changes, and they are widely distributed throughout the structure of NPC1 (Figure  
165 1A). Using the co-structure of full-length NPC1 and EBOV dGP [16], we identified 10  
166 missense SNPs in 8 amino acid positions located in the interface (i.e., 2 loop structures at  
167 amino acid positions 419-428 and 500-508) with EBOV GP (Figure 1B).

168

169 **Human NPC1 polymorphisms affecting filovirus entry into cells**

170 We next established an NPC1 knockout Vero E6 cell line, Vero E6/NPC1-KO  
171 cl.19 (Supplementary Figure 1A and B), and confirmed that its susceptibility to VSV $\Delta$ G-  
172 EBOV, rVSV-EBOV, and EBOV-GFP was completely abolished (Supplementary Figure  
173 1C-E). The Vero E6/NPC1-KO cl.19 cells were then transduced with a retroviral vector  
174 resulting in eleven different cell lines stably expressing wild-type human NPC1 (293T-  
175 NPC1) or NPC1 SNP mutants (I419V, I419F, Y420S, Y420H, P424A, S425L, A427T,  
176 G500E, D502E, and D508N). Introducing the wild-type NPC1 gene into the knockout  
177 cells completely restored the susceptibility to filovirus entry and infection  
178 (Supplementary Figure 1C-E), as has been shown with NPC1-deficient CHO and reptile-  
179 derived cells [10, 12]. Transcription and expression levels of the transduced NPC1 genes  
180 were examined by quantitative PCR and western blot analyses, respectively (see  
181 Supplementary Materials and Methods). In all of the NPC1 SNP mutant cell lines,  
182 expression levels of NPC1 were equivalent to or higher than those of 293T-NPC1-  
183 expressing cells (Supplementary Figure 2). We also confirmed that these NPC1s were

184 similarly localized at endosomal vesicles (data not shown).

185 To evaluate whether these SNP substitutions affected the efficiency of viral entry,  
186 each cell line was infected with replication-incompetent VSV pseudotyped with filovirus  
187 GPs, and relative IUs were compared among the cell lines (Figure 2). We found that  
188 P424A, S425L, D502E, and D508N substitutions in NPC1 reduced the entry of VSV  
189 pseudotyped with GPs from multiple filovirus species. P424A and D508N substitutions  
190 significantly affected the entry of VSV $\Delta$ G- EBOV, - BDBV, - TAFV, - SUDV, - RESTV,  
191 and - LLOV, but not MARV and/or -RAVV. On the other hand, S425L and D502E  
192 substitutions reduced the entry of VSV $\Delta$ G-MARV, -and some of the pseudotyped VSV  
193 with ebolavirus GPs. Y420S substitution only reduced the entry of VSV $\Delta$ G-LLOV. It  
194 was noted that these substitutions resulted in different patterns of reduction  
195 corresponding to the filovirus genera (i.e., *Ebolavirus*, *Marburgvirus*, and *Cuevavirus*).  
196 In particular, P424A/D508N and S425L/D502E substitutions seemed to be important for  
197 the reduced entry of VSVs pseudotyped with ebolavirus and marburgvirus GPs,  
198 respectively. In some cell lines, infectivity of the viruses was enhanced and it was  
199 correlated with relatively high expression levels of NPC1 (Supplementary Figure 2).

#### 200 201 **Reduced plaque-forming ability of rVSV-EBOV in Vero E6 cells expressing NPC1** 202 **with P424A or D508N substitution**

203 We then compared the plaque-forming abilities of rVSV-EBOV and  
204 rVSV-MARV using the same cell lines (Figure 3). Although statistically significant  
205 difference was not observed, the P424A and S425L substitutions moderately reduced the  
206 plaque number of rVSV-EBOV and rVSV-MARV, respectively (Figure  
207

208 3A). As expected, the average plaque sizes of rVSV-EBOV in cells expressing NPC1  
209 with the D508N substitution were significantly smaller than in 293T-NPC1-  
210 expressing cells and the P424A substitution also slightly reduced the plaque size (Figure  
211 3B). Consistent with the data shown in Figure 2, rVSV-MARV formed slightly, but not  
212 significantly, smaller plaques in the cell line expressing S425L NPC1 (Figure 3B).

213

#### 214 **Reduced focus-forming ability of EBOV in Vero E6 cells with the P424A substitution**

215 To examine the effects of substitutions associated with NPC1 SNPs on  
216 actual filovirus infection, we used an infectious EBOV expressing GFP and determined  
217 the viral focus numbers and average focus size in each cell line. Consistent with our  
218 pseudotyped VSV data, the P424A substitution resulted in reduced focus numbers  
219 of EBOV-GFP (Figure 3C). The average size of foci in this cell line was also  
220 significantly smaller than in cells expressing 293T-NPC1 (Figure 3D). Although  
221 these differences were not significant in a multiple comparison analysis, Welch's t-test  
222 gave significant differences compared to 293T-NPC1-expressing cells. The D508N  
223 substitution slightly reduced the focus size of EBOV-GFP but there was no statistically  
224 significant difference compared to 293T-NPC1-expressing cells.

225

226

227

228 **DISCUSSION**

229           With human immunodeficiency virus type 1 (HIV-1) infection, there is a subset  
230 of people who are inherently resistant to the virus [28-31]. In particular, genetic variation  
231 in the host viral receptors has been shown to reduce the susceptibility to HIV infection in  
232 humans [28, 29]. Though asymptomatic filovirus infection is less studied, Baron et al.  
233 [32] reported potential asymptomatic cases during the outbreak in Sudan in 1979, and  
234 Dean et al. [33] estimated the proportion of asymptomatic transmissions during the recent  
235 epidemic in West Africa. Although host genetics and Ebola virus disease progression and  
236 resistance have been studied in mice [34, 35], the details of genetic polymorphisms that  
237 may affect susceptibility of humans to filoviruses have not been elucidated yet.

238           In the present study, we focused on ten reported NPC1 SNP substitutions that  
239 interface with GP. Although none of the SNPs tested here completely ablated viral entry  
240 or infectivity, some SNPs were nevertheless found to be important for filovirus infection.  
241 In our experiments, P424A substitution reduced entry of VSV pseudotyped with  
242 ebolavirus but not marburgvirus GPs. Moreover, focus sizes of EBOV-GFP were also  
243 reduced in this cell line. Interestingly, Wang et al. [15] demonstrated that the P424A  
244 NPC1 mutant retained binding capacity to dGP but with reduced affinity compared to  
245 wild-type NPC1. Taken together, these findings suggest that the P424A substitution in  
246 NPC1 lowers its binding capacity to dGP, resulting in reduced viral entry and infection.

247           S425L substitution also reduced the infection with some pseudotyped VSVs,  
248 including VSV $\Delta$ G-MARV and -RAVV. The serine residue at position 425 in NPC1 was  
249 shown to be involved in the interaction with the amino acid residue at position 142 of the  
250 EBOV GP molecule [15]. However, since amino acid residues at this position are different  
251 in EBOV and MARV GPs (serine at 142 of EBOV GP and glutamine at 126 of MARV

252 GP, respectively), the effects of S425L substitution might be different between EBOV and  
253 MARV. It has also been demonstrated that single amino acid mutations at positions 502  
254 or 503 in NPC1 can reduce viral infection [13, 14]. Our experiments confirmed this  
255 finding as D502E substitution reduced the entry of some of the pseudotyped viruses we  
256 tested and also reduced infection with EBOV-GFP (although not significantly). Notably,  
257 while the previous study introduced a significant loss of charge at residue 502 by mutating  
258 the aspartic acid to phenylalanine [13], our study shows that even minimal variation at  
259 this residue (D to E) can have an effect on viral entry.

260           Some other amino acids that are also important for binding to dGP have not been  
261 reported as SNP sites in the NPC1 loops [15]. The rapidly increasing sequence data in  
262 public databases may hereafter provide additional information on NPC1 SNP  
263 substitutions not evaluated in this study. It is also of interest to investigate multiple SNP  
264 substituins in the loops. Although more sensitive studies are needed to further assess the  
265 capacity for NPC1 variation to influence filovirus infection, identifying genetic variations  
266 that affect the susceptibility of hosts to filoviruses will be crucial in understanding  
267 filovirus disease progression and host cell-restriction.

268

269



270 **Supplementary Data**

271 Supplementary materials are available at The Journal of Infectious Diseases online.  
272 Consisting of data provided by the authors to benefit the reader, the posted materials are  
273 not copyedited and are the sole responsibility of the authors, so questions or comments  
274 should be addressed to the corresponding author.

275

276 **Notes**

277 *Acknowledgments.* The authors would like to thank GE Healthcare Japan Corporation  
278 and Koshin Kagaku K.K. for their assistance in the establishment of the IN Cell Analyzer  
279 2000 protocol, Life Technologies Japan, Ltd. and Frontier Science co., Ltd. for  
280 their assistance in gene editing, and Kim Barrymore for editing the manuscript. The  
281 authors would also like to thank Michihito Sasaki (Division of Molecular Pathobiology,  
282 Research Center for Zoonosis Control, Hokkaido University) for anti-LAMP1 antibody.

283

284 **References**

- 285 1. Kuhn JH. Guide to the correct use of filoviral nomenclature. *Curr Top Microbiol*  
286 *Immunol* **2017**; 411:447-460.
- 287 2. Takada A, Robison C, Goto H, et al. A system for functional analysis of Ebola virus  
288 glycoprotein. *Proceedings of the National Academy of Sciences of the United States*  
289 *of America* **1997**; 94:14764-9.
- 290 3. Hofmann-Winkler H, Kaup F, Pöhlmann S. Host cell factors in filovirus entry: Novel  
291 players, new insights. *Viruses* **2012**; 4:3336-62.
- 292 4. Takada A. Filovirus tropism: cellular molecules for viral entry. *Front Microbiol* **2012**;  
293 3:34.
- 294 5. Nanbo A, Imai M, Watanabe S, et al. Ebolavirus is internalized into host cells via  
295 macropinocytosis in a viral glycoprotein-dependent manner. *PLoS Pathog* **2010**;  
296 6:e1001121.
- 297 6. Saeed MF, Kolokoltsov AA, Albrecht T, Davey RA. Cellular entry of Ebola virus  
298 involves uptake by a macropinocytosis-like mechanism and subsequent trafficking  
299 through early and late endosomes. *PLoS Pathog* **2010**; 6:e1001110.
- 300 7. Aleksandrowicz P, Marzi A, Biedenkopf N, et al. Ebola virus enters host cells by  
301 macropinocytosis and clathrin-mediated endocytosis. *J Infect Dis* **2011**; 204 Suppl  
302 3:S957-67.
- 303 8. Chandran K, Sullivan NJ, Felbor U, Whelan SP, Cunningham JM. Endosomal  
304 proteolysis of the Ebola virus glycoprotein is necessary for infection. *Science* **2005**;  
305 308:1643-5.
- 306 9. Misasi J, Chandran K, Yang J-Y, et al. Filoviruses require endosomal cysteine  
307 proteases for entry but exhibit distinct protease preferences. *J Virol* **2012**; 86:3284-

- 308 92.
- 309 10. Carette JE, Raaben M, Wong AC, et al. Ebola virus entry requires the cholesterol  
310 transporter Niemann-Pick C1. *Nature* **2011**; 477:340-3.
- 311 11. Cote M, Misasi J, Ren T, et al. Small molecule inhibitors reveal Niemann-Pick C1 is  
312 essential for Ebola virus infection. *Nature* **2011**; 477:344-8.
- 313 12. Miller EH, Obernosterer G, Raaben M, et al. Ebola virus entry requires the host-  
314 programmed recognition of an intracellular receptor. *EMBO J* **2012**; 31:1947-60.
- 315 13. Ng M, Ndungo E, Kaczmarek ME, et al. Filovirus receptor NPC1 contributes to  
316 species-specific patterns of ebolavirus susceptibility in bats. *eLife* **2015**;4:e11785.
- 317 14. Ndungo E, Herbert AS, Raaben M, et al. A single residue in Ebola virus receptor  
318 NPC1 influences cellular host range in reptiles. *mSphere* **2016**; 1: e00007-16.
- 319 15. Wang H, Shi Y, Song J, et al. Ebola viral glycoprotein bound to its endosomal  
320 receptor Niemann-Pick C1. *Cell* **2016**; 164:258-68.
- 321 16. Gong X, Qian HW, Zhou XH, et al. Structural insights into the Niemann-Pick C1  
322 (NPC1)-mediated cholesterol transfer and Ebola infection. *Cell* **2016**; 165:1467-78.
- 323 17. Takada A, Feldmann H, Stroehrer U, et al. Identification of protective epitopes on  
324 Ebola virus glycoprotein at the single amino acid level by using recombinant  
325 vesicular stomatitis viruses. *J Virol* **2003**; 77:1069-74.
- 326 18. Ebihara H, Theriault S, Neumann G, et al. In vitro and in vivo characterization of  
327 recombinant Ebola viruses expressing enhanced green fluorescent protein. *J Infect*  
328 *Dis* **2007**; 196 Suppl 2:S313-22.
- 329 19. Furuyama W, Miyamoto H, Yoshida R, Takada A. Quantification of filovirus  
330 glycoprotein-specific antibodies. *Methods Mol Biol (Clifton, NJ)* **2017**; 1628:309-  
331 20.

- 332 20. Maruyama J, Miyamoto H, Kajihara M, et al. Characterization of the envelope  
333 glycoprotein of a novel filovirus, Lloviu virus. *J Virol* **2014**; 88:99-109.
- 334 21. Kajihara M, Nakayama E, Marzi A, Igarashi M, Feldmann H, Takada A. Novel  
335 mutations in Marburg virus glycoprotein associated with viral evasion from antibody  
336 mediated immune pressure. *J Gen Virol* **2013**; 94:876-83.
- 337 22. Ebihara H, Yoshimatsu K, Ogino M, et al. Pathogenicity of Hantaan virus in newborn  
338 mice: genetic reassortant study demonstrating that a single amino acid change in  
339 glycoprotein G1 is related to virulence. *J Virol* **2000**; 74:9245-55.
- 340 23. Kitamura T, Koshino Y, Shibata F, et al. Retrovirus-mediated gene transfer and  
341 expression cloning: Powerful tools in functional genomics. *Exp Hematol* **2003**;  
342 31:1007-14.
- 343 24. Liang XQ, Potter J, Kumar S, et al. Rapid and highly efficient mammalian cell  
344 engineering via Cas9 protein transfection. *J Biotechnol* **2015**; 208:44-53.
- 345 25. Yu X, Liang XQ, Xie HM, et al. Improved delivery of Cas9 protein/gRNA complexes  
346 using lipofectamine CRISPRMAX. *Biotechnol Lett.* **2016**; 38:919-29.
- 347 26. Kuroda M, Fujikura D, Nanbo A, et al. Interaction between TIM-1 and NPC1 is  
348 important for the cellular entry of Ebola virus. *J Virol* **2015**; 89:6481-93.
- 349 27. Team RC. R: A Language and environment for statistical computing. R foundation  
350 for statistical computing, Vienna, Austria **2015**; URL <https://www.R-project.org/>
- 351 28. Liu R, Paxton WA, Choe S, et al. Homozygous defect in HIV-1 coreceptor accounts  
352 for resistance of some multiply-exposed individuals to HIV-1 infection. *Cell* **1996**;  
353 86:367-77.
- 354 29. Samson M, Libert F, Doranz BJ, et al. Resistance to HIV-1 infection in Caucasian  
355 individuals bearing mutant alleles of the CCR-5 chemokine receptor gene. *Nature*

- 356        **1996**; 382:722-5.
- 357    30. O'Brien SJ, Moore JP. The effect of genetic variation in chemokines and their  
358        receptors on HIV transmission and progression to AIDS. *Immunol Rev* **2000**; 177:99-  
359        111.
- 360    31. Pereyra F, Addo MM, Kaufmann DE, et al. Genetic and immunologic heterogeneity  
361        among persons who control HIV infection in the absence of therapy. *J Infect Dis*  
362        **2008**; 197:563-71.
- 363    32. Baron RC, McCormick JB, Zubeir OA. Ebola virus disease in southern Sudan:  
364        hospital dissemination and intrafamilial spread. *Bull World Health Organ* **1983**;  
365        61:997-1003.
- 366    33. Dean NE, Halloran ME, Yang Y, Longini IM. The transmissibility and pathogenicity  
367        of Ebola virus: a systematic review and meta-analysis of household secondary attack  
368        rate and asymptomatic infection. *Clin Infect Dis* **2016**; 62:1277-1286.
- 369    34. Rasmussen AL, Okumura A, Ferris MT, et al. Host genetic diversity enables Ebola  
370        hemorrhagic fever pathogenesis and resistance. *Science* **2014**; 346:987-91.
- 371    35. Hill-Batorski L, Halfmann P, Marzi A, et al. Loss of interleukin 1 receptor antagonist  
372        enhances susceptibility to Ebola virus infection. *J Infect Dis* **2015**; 212 Suppl 2:S329-  
373        35.
- 374
- 375

376 **Figure Legends**

377

378 **Figure 1. Structural-guided approach to human NPC1 SNP selection.**

379 A, 222 missense SNPs are represented in black on the structure from NPC1. B, Co-  
380 structure of EBOV GP (blue) and NPC1 (tan) with amino acid positions of SNPs indicated  
381 in red (PDB: 5JNX) [16].

382

383 **Figure 2. Infectivities of VSV pseudotyped with filovirus GPs in Vero E6 cell lines.**

384 Confluent monolayers of each cell line grown in 96-well plates were infected with  
385 VSV $\Delta$ G-EBOV, VSV $\Delta$ G-BDBV, VSV $\Delta$ G-TAFV, VSV $\Delta$ G-SUDV, VSV $\Delta$ G-RESTV,  
386 VSV $\Delta$ G-MARV, VSV $\Delta$ G-RAVV, and VSV $\Delta$ G-LLOV. Twenty hours later, the virus  
387 infectious unit (IU) in each cell line was determined by counting the number of GFP-  
388 expressing cells with an IN Cell Analyzer 2000 (GE Healthcare). Relative infectivity in  
389 each cell line was calculated by setting the IU value given by Vero E6 cells expressing  
390 293T-NPC1 (approximately 1000-3000 IU/well for each assay) to 100%. Means and  
391 standard errors of thirty replicates are shown. Values significantly lower than for 293T-  
392 NPC1 are indicated (\* $P < 0.05$ , \*\* $P < 0.01$ , \*\*\* $P < 0.001$ ).

393

394 **Figure 3. Plaque/focus formation of rVSV-EBOV, rVSV-MARV, and EBOV-GFP in**  
395 **Vero E6 cell lines**

396 A, rVSV-EBOV and rVSV-MARV (multiplicity of infection = 0.0005 in Vero E6 cells)  
397 were inoculated into Vero E6 cells grown in 6-well tissue culture plates. After adsorption  
398 for 1 hour, the inoculum was removed and the cells were overlaid with Eagle's minimal  
399 essential medium containing 1.0% Bacto Agar (BD) and then incubated for 3 days at

400 37°C. Cells were stained with 0.5 % crystal violet in 10% formalin and the plaque-  
401 forming unit (PFU) in each cell line was determined by counting the number of all visible  
402 plaques per well (i.e., 50-100 plaques for each assay). Data represent means and standard  
403 errors of at least three independent experiments. *B*, Plaque sizes were measured with  
404 Image-J software. Means and standard errors of 50-100 plaques per well are shown. *C*,  
405 EBOV-GFP (multiplicity of infection = 0.002 in Vero E6 cells) were inoculated into  
406 confluent monolayers of Vero E6 cells grown in 96-well tissue culture plates. After  
407 adsorption for 1 hour, the inoculum was replaced with Eagle's minimal essential medium  
408 containing 1.2% carboxymethyl cellulose. After incubation for 3 days at 37°C, the cells  
409 were fixed and GFP foci in each cell line were counted under a fluorescence microscope.  
410 Data represent means and standard errors of triplicate assays. *D*, Focus sizes were  
411 measured with Image-J software. Means and standard errors of 60-150 foci per well are  
412 shown. (*A-D*) Values significantly lower than for 293T-NPC1 are indicated (\* $P < 0.05$ ,  
413 \*\* $P < 0.01$ , \*\*\* $P < 0.001$ ).

414

## Supplementary Materials and Methods

### Establishment of Vero E6/NPC1-KO

We found a candidate gRNA target sequence in the genomic region of Vero E6 NPC1 and designed oligonucleotides (CRISPR-VeroNPC1-F1: 5'-TAATACGACTCACTATAGCTGCTACTGTGTCCGGCGC-3' and CRISPR-VeroNPC1-R1: 5'-TTCTAGCTCTAAAACGCGCCGGACACAGTAGCAG-3') by using the CRISPRdirect web tool [1] (<https://crispr.dbcls.jp/>). Synthesis of a gRNA template, in vitro transcription of gRNA, and purification of gRNA products were performed using the GeneArt precision gRNA synthesis kit (Invitrogen) according to the manufacturer's instructions. Vero E6 cells were transfected with gRNA products and the Platinum Cas9 nuclease (Invitrogen) mixture using Lipofectamine CRISPRMAX Cas9 Transfection Reagent (Invitrogen) according to the manufacturer's instructions, followed by incubation for 3 days at 37°C. By genomic cleavage detection assay with a specific primer set (VeroNPC1-367F: 5'-CTGAGGAGAAGGGCAAAG-3' and VeroNPC1-846R: 5'-CATCGCTAGACCAACTTCC-3') using a GeneArt Genomic Cleavage Detection Kit (Invitrogen), we confirmed a cleaved DNA product of 426 base pairs induced by the gRNA introduction into cells. We retreated the transfected Vero E6 cells with Cas9 nuclease solution and the gRNA to generate double knockout cells. For clonal isolation, the transfected cell suspension (5 cells/ml) was seeded on 96-well plates precoated with poly D-lysine (Nunc). After clonal expansion for 3 weeks, we obtained 97 clones. Cells from each well were harvested, followed by western blotting to confirm that there was no expression of NPC1. Of the 97 clones examined, we selected 2 (Vero E6/NPC1-KO cl. 19 and cl. 89) and used cl. 19 for the following experiments.

### Generation of each NPC1-expressing cell line

To generate the retrovirus, Plat-GP cells were cotransfected with pMXs-puro [2] encoding HEK293T NPC1 or cDNA of each NPC1 mutant and the expression plasmid pCAGGS [3] encoding VSV-G cDNA with FuGENE HD transfection reagent (Promega) according to the manufacturer's recommendations. Two days later, culture supernatants containing retroviruses were collected, clarified through 0.45- $\mu$ m filters, and inoculated into Vero E6/NPC1-KO cl. 19 cells. Cell lines stably expressing each NPC1 SNP were selected with DMEM containing 10% FCS and 20  $\mu$ g/ml puromycin (Sigma-Aldrich).

### SDS-PAGE and western blotting

Cells ( $2 \times 10^6$  cells for each cell line) were lysed with 100  $\mu$ l of NTE-CHAPS

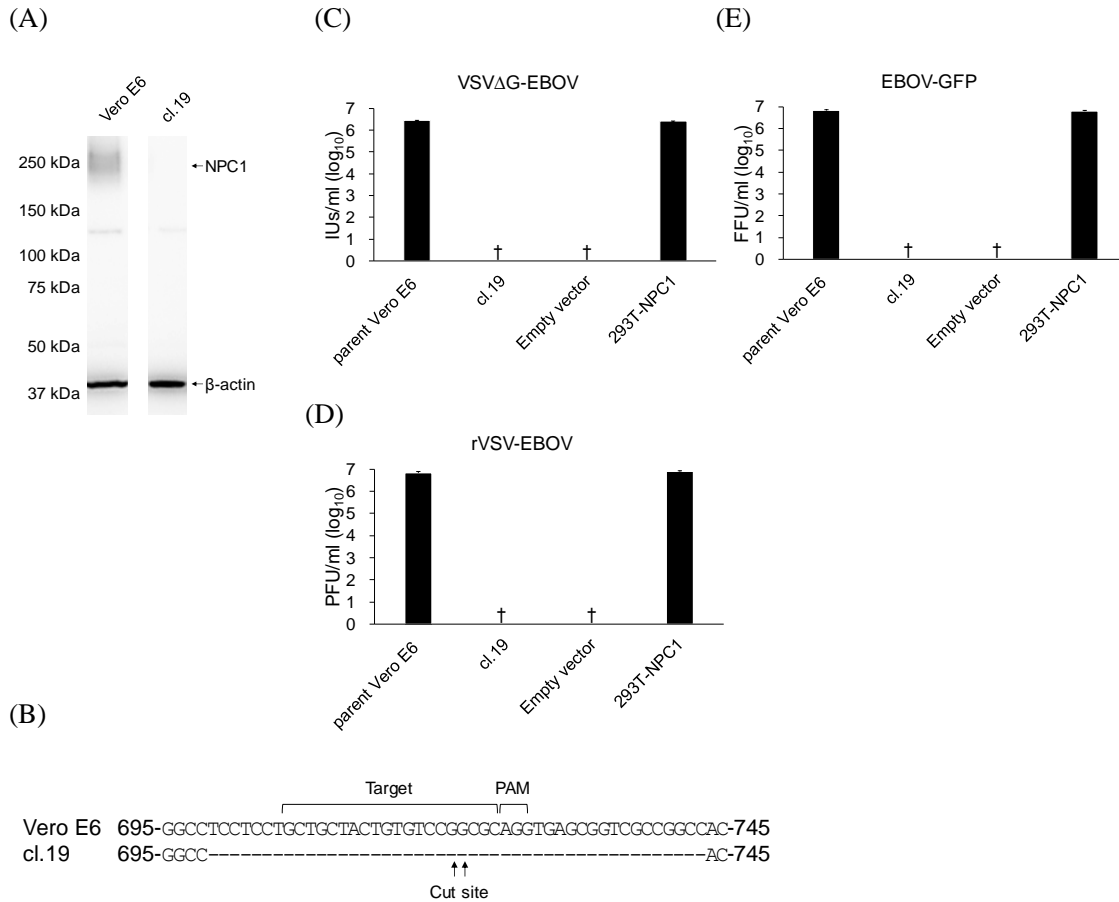


buffer (10 mM Tris-HCl [pH 7.5], 140 mM NaCl, 1 mM EDTA, 0.5% wt/vol CHAPS) [4] containing a protease inhibitor mixture (Roche). To facilitate disruption of cells, cell suspensions were frozen at -80°C. Samples were centrifuged at 4°C, 10000×g for 10 min. Supernatants were mixed with sodium dodecyl sulfate (SDS)-PAGE sample buffer (Bio-Rad) with 10% 2-mercaptoethanol and incubated at 65°C for 15 min. Expressed proteins were separated in SDS-polyacrylamide gels (SuperSep Ace 5-20%, Wako) and transferred to polyvinylidene fluoride (PVDF) membranes (Merck). PBS containing 3% (wt/vol) skim milk (BD) and PBS containing 0.05% (vol/vol) Tween 20 (PBST) were used as blocking and wash buffers, respectively. The PVDF membranes were incubated with an anti-Niemann Pick C1 rabbit antibody (abcam, ab108921) recognizing the polypeptide containing amino acid residues from position 1250 to the C-terminus of human NPC1 and anti-β actin mouse monoclonal antibody (abcam, ab6276) for 60 min, washed with PBST, and then incubated with horseradish peroxidase (HRP)-conjugated goat anti-mouse IgG (Jackson ImmunoResearch, 115-035-062) and HRP-conjugated goat anti-rabbit IgG (KPL, 074-1506) for 60 min. After washing with PBST, the bound antibodies were visualized with Immobilon Western (Millipore). Relative expression levels were analyzed with Amersham Imager 600 Software (GE Healthcare).

### **Real-time PCR**

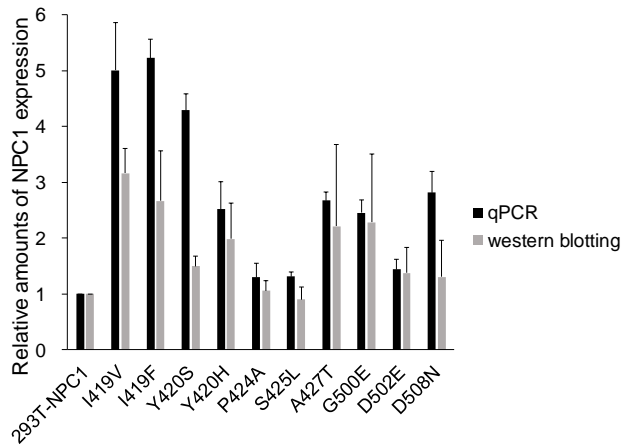
To compare the transcription levels of the NPC1 genes in the stable cell lines, the copy numbers of NPC1 mRNA were analyzed with real-time PCR using the comparative CT method in a Quant Studio 3 (Applied Biosystems). RNA extraction and reverse transcription from cultured cell lysates were conducted using a Power SYBR® Green Cells-to-CT Kit (Applied Biosystems) and real-time PCR mixtures were prepared with PowerUp™ SYBR™ Green Master Mix (Applied Biosystems) and 0.4 μM primers (HEK293T-NPC1-2987F: 5'-TGAGATTCCTGCCCATGTTC-3'; HEK293T-NPC1-3086R: 5'-TGGCCAAGGAGGATGTAAAC-3'; hum\_b-actin-270F: 5'-TTCTACAATGAGCTGCGTGTG-3'; hum\_b-actin-389R: 5'-GGGGTGTTGAAGGTCTCAAA-3'). PCR reactions were performed according to the manufacturer's instructions.

## Supplementary Figures



### Supplementary Figure 1. Generation of Vero E6/NPC1-KO cells and its susceptibility to VSV $\Delta$ G-EBOV, rVSV-EBOV, and EBOV-GFP

(A) Expression of NPC1 in parent Vero E6 and Vero E6/NPC1-KO clone 19 (cl. 19) cells was analyzed by western blotting. The experiment was performed three times and representative data are shown. (B) Deletion of the desired region of the NPC1 gene in cl. 19 cells were confirmed by DNA sequencing. (C-E) Parent Vero E6, cl. 19, cl. 19 transduced with an empty vector, and cl. 19 stably expressing 293T-NPC1 were infected with VSV $\Delta$ G-EBOV (C), rVSV-EBOV (D), or EBOV-GFP (E). Data represent means and standard errors of triplicate assays. †: Not detected.



## Supplementary Figure 2. Transcription and expression levels of NPC1 in each stable cell line

Transcription levels of NPC1 mRNAs were analyzed with qPCR and western blotting. Data represent means and standard deviations of at least three independent experiments. The rank correlation coefficient of spearman ( $r_s$ ) showed that transcription and expression levels of NPC1 were significantly correlated ( $r_s = 0.63$ ,  $P$ -value = 0.000073).

### References

1. Naito Y, Hino K, Bono H, Ui-Tei K. CRISPRdirect: software for designing CRISPR/Cas guide RNA with reduced off-target sites. *Bioinformatics* **2014**; 31:1120-3.
2. Kitamura T, Koshino Y, Shibata F, et al. Retrovirus-mediated gene transfer and expression cloning: Powerful tools in functional genomics. *Exp Hematol* **2003**; 31:1007-14.
3. Niwa H, Yamamura K, Miyazaki J. Efficient selection for high-expression transfectants with a novel eukaryotic vector. *Gene* **1991**; 108:193-9.
4. Miller EH, Obernosterer G, Raaben M, et al. Ebola virus entry requires the host-programmed recognition of an intracellular receptor. *EMBO J* **2012**; 31:1947-60.

## Supplementary Materials and Methods

### Establishment of Vero E6/NPC1-KO

We found a candidate gRNA target sequence in the genomic region of Vero E6 NPC1 and designed oligonucleotides (CRISPR-VeroNPC1-F1: 5'-TAATACGACTCACTATAGCTGCTACTGTGTCCGGCGC-3' and CRISPR-VeroNPC1-R1: 5'-TTCTAGCTCTAAAACGCGCCGGACACAGTAGCAG-3') by using the CRISPRdirect web tool [1] (<https://crispr.dbcls.jp/>). Synthesis of a gRNA template, in vitro transcription of gRNA, and purification of gRNA products were performed using the GeneArt precision gRNA synthesis kit (Invitrogen) according to the manufacturer's instructions. Vero E6 cells were transfected with gRNA products and the Platinum Cas9 nuclease (Invitrogen) mixture using Lipofectamine CRISPRMAX Cas9 Transfection Reagent (Invitrogen) according to the manufacturer's instructions, followed by incubation for 3 days at 37°C. By genomic cleavage detection assay with a specific primer set (VeroNPC1-367F: 5'-CTGAGGAGAAGGGCAAAG-3' and VeroNPC1-846R: 5'-CATCGCTAGACCAACTTCC-3') using a GeneArt Genomic Cleavage Detection Kit (Invitrogen), we confirmed a cleaved DNA product of 426 base pairs induced by the gRNA introduction into cells. We retreated the transfected Vero E6 cells with Cas9 nuclease solution and the gRNA to generate double knockout cells. For clonal isolation, the transfected cell suspension (5 cells/ml) was seeded on 96-well plates precoated with poly D-lysine (Nunc). After clonal expansion for 3 weeks, we obtained 97 clones. Cells from each well were harvested, followed by western blotting to confirm that there was no expression of NPC1. Of the 97 clones examined, we selected 2 (Vero E6/NPC1-KO cl. 19 and cl. 89) and used cl. 19 for the following experiments.

### Generation of each NPC1-expressing cell line

To generate the retrovirus, Plat-GP cells were cotransfected with pMXs-puro [2] encoding HEK293T NPC1 or cDNA of each NPC1 mutant and the expression plasmid pCAGGS [3] encoding VSV-G cDNA with FuGENE HD transfection reagent (Promega) according to the manufacturer's recommendations. Two days later, culture supernatants containing retroviruses were collected, clarified through 0.45- $\mu$ m filters, and inoculated into Vero E6/NPC1-KO cl. 19 cells. Cell lines stably expressing each NPC1 SNP were selected with DMEM containing 10% FCS and 20  $\mu$ g/ml puromycin (Sigma-Aldrich).

### SDS-PAGE and western blotting

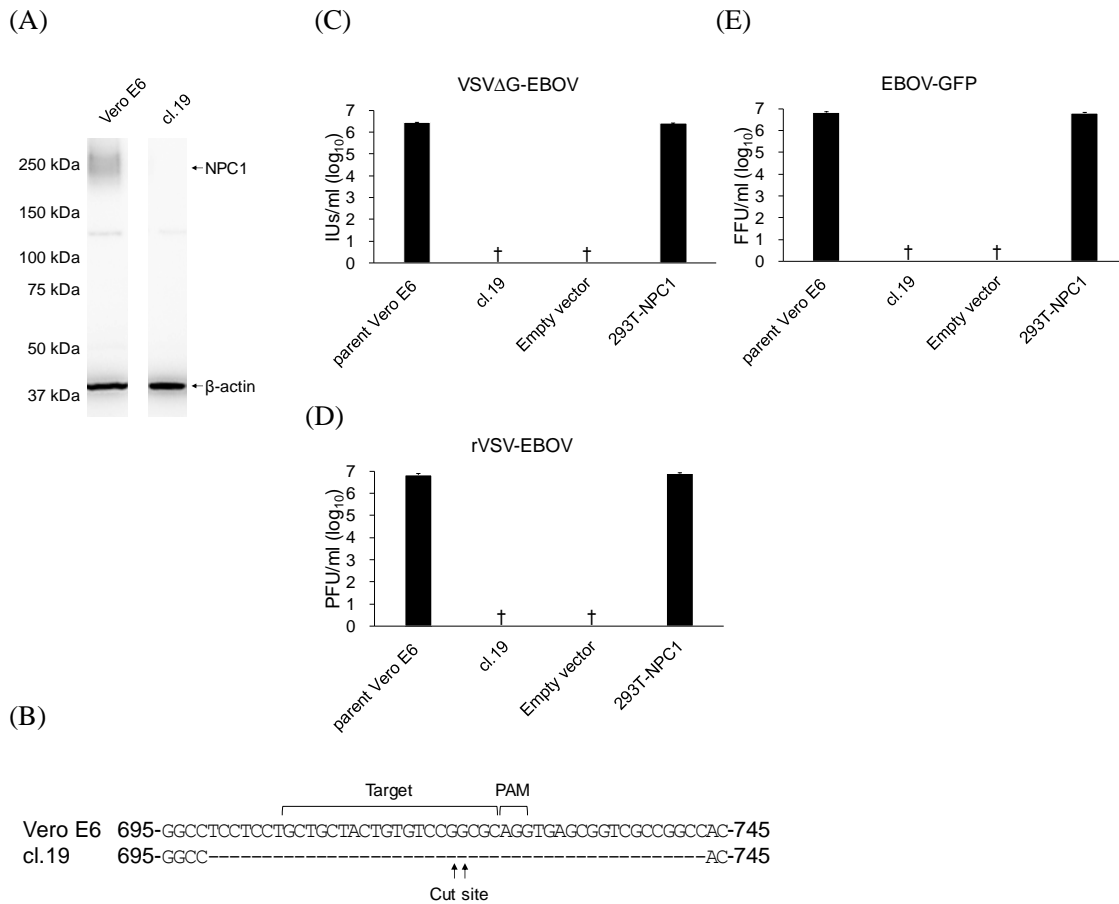
Cells ( $2 \times 10^6$  cells for each cell line) were lysed with 100  $\mu$ l of NTE-CHAPS

buffer (10 mM Tris-HCl [pH 7.5], 140 mM NaCl, 1 mM EDTA, 0.5% wt/vol CHAPS) [4] containing a protease inhibitor mixture (Roche). To facilitate disruption of cells, cell suspensions were frozen at -80°C. Samples were centrifuged at 4°C, 10000×g for 10 min. Supernatants were mixed with sodium dodecyl sulfate (SDS)-PAGE sample buffer (Bio-Rad) with 10% 2-mercaptoethanol and incubated at 65°C for 15 min. Expressed proteins were separated in SDS-polyacrylamide gels (SuperSep Ace 5-20%, Wako) and transferred to polyvinylidene fluoride (PVDF) membranes (Merck). PBS containing 3% (wt/vol) skim milk (BD) and PBS containing 0.05% (vol/vol) Tween 20 (PBST) were used as blocking and wash buffers, respectively. The PVDF membranes were incubated with an anti-Niemann Pick C1 rabbit antibody (abcam, ab108921) recognizing the polypeptide containing amino acid residues from position 1250 to the C-terminus of human NPC1 and anti-β actin mouse monoclonal antibody (abcam, ab6276) for 60 min, washed with PBST, and then incubated with horseradish peroxidase (HRP)-conjugated goat anti-mouse IgG (Jackson ImmunoResearch, 115-035-062) and HRP-conjugated goat anti-rabbit IgG (KPL, 074-1506) for 60 min. After washing with PBST, the bound antibodies were visualized with Immobilon Western (Millipore). Relative expression levels were analyzed with Amersham Imager 600 Software (GE Healthcare).

### **Real-time PCR**

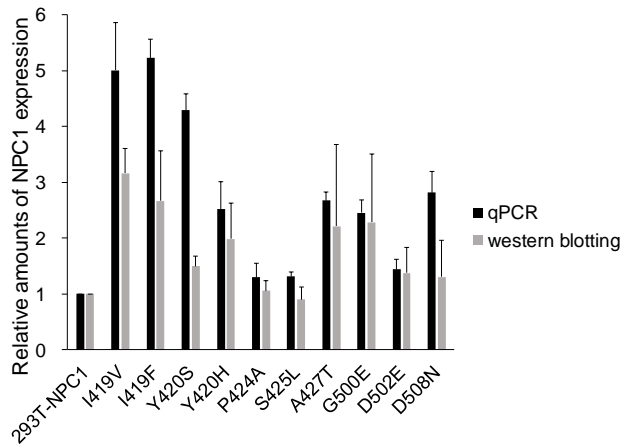
To compare the transcription levels of the NPC1 genes in the stable cell lines, the copy numbers of NPC1 mRNA were analyzed with real-time PCR using the comparative CT method in a Quant Studio 3 (Applied Biosystems). RNA extraction and reverse transcription from cultured cell lysates were conducted using a Power SYBR® Green Cells-to-CT Kit (Applied Biosystems) and real-time PCR mixtures were prepared with PowerUp™ SYBR™ Green Master Mix (Applied Biosystems) and 0.4 μM primers (HEK293T-NPC1-2987F: 5'-TGAGATTCCTGCCCATGTTC-3'; HEK293T-NPC1-3086R: 5'-TGGCCAAGGAGGATGTAAAC-3'; hum\_b-actin-270F: 5'-TTCTACAATGAGCTGCGTGTG-3'; hum\_b-actin-389R: 5'-GGGGTGTTGAAGGTCTCAAA-3'). PCR reactions were performed according to the manufacturer's instructions.

## Supplementary Figures



### Supplementary Figure 1. Generation of Vero E6/NPC1-KO cells and its susceptibility to VSV $\Delta$ G-EBOV, rVSV-EBOV, and EBOV-GFP

(A) Expression of NPC1 in parent Vero E6 and Vero E6/NPC1-KO clone 19 (cl. 19) cells was analyzed by western blotting. The experiment was performed three times and representative data are shown. (B) Deletion of the desired region of the NPC1 gene in cl. 19 cells were confirmed by DNA sequencing. (C-E) Parent Vero E6, cl. 19, cl. 19 transduced with an empty vector, and cl. 19 stably expressing 293T-NPC1 were infected with VSV $\Delta$ G-EBOV (C), rVSV-EBOV (D), or EBOV-GFP (E). Data represent means and standard errors of triplicate assays. †: Not detected.



## Supplementary Figure 2. Transcription and expression levels of NPC1 in each stable cell line

Transcription levels of NPC1 mRNAs were analyzed with qPCR and western blotting. Data represent means and standard deviations of at least three independent experiments. The rank correlation coefficient of spearman ( $r_s$ ) showed that transcription and expression levels of NPC1 were significantly correlated ( $r_s = 0.63$ ,  $P$ -value = 0.000073).

### References

1. Naito Y, Hino K, Bono H, Ui-Tei K. CRISPRdirect: software for designing CRISPR/Cas guide RNA with reduced off-target sites. *Bioinformatics* **2014**; 31:1120-3.
2. Kitamura T, Koshino Y, Shibata F, et al. Retrovirus-mediated gene transfer and expression cloning: Powerful tools in functional genomics. *Exp Hematol* **2003**; 31:1007-14.
3. Niwa H, Yamamura K, Miyazaki J. Efficient selection for high-expression transfectants with a novel eukaryotic vector. *Gene* **1991**; 108:193-9.
4. Miller EH, Obernosterer G, Raaben M, et al. Ebola virus entry requires the host-programmed recognition of an intracellular receptor. *EMBO J* **2012**; 31:1947-60.

Figure 1

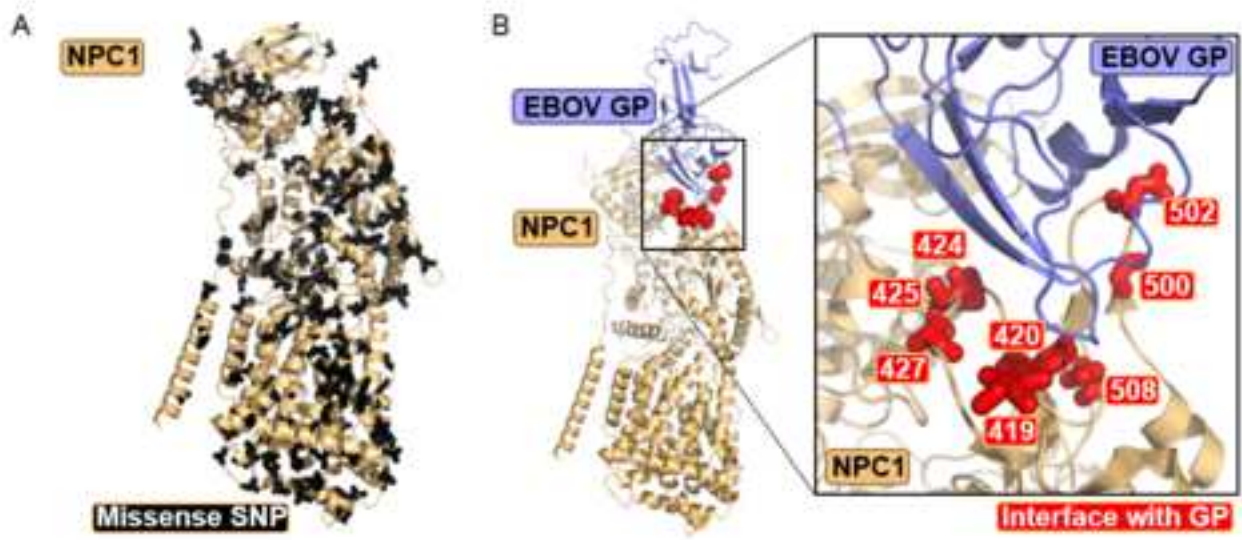


Figure 1



Figure 2

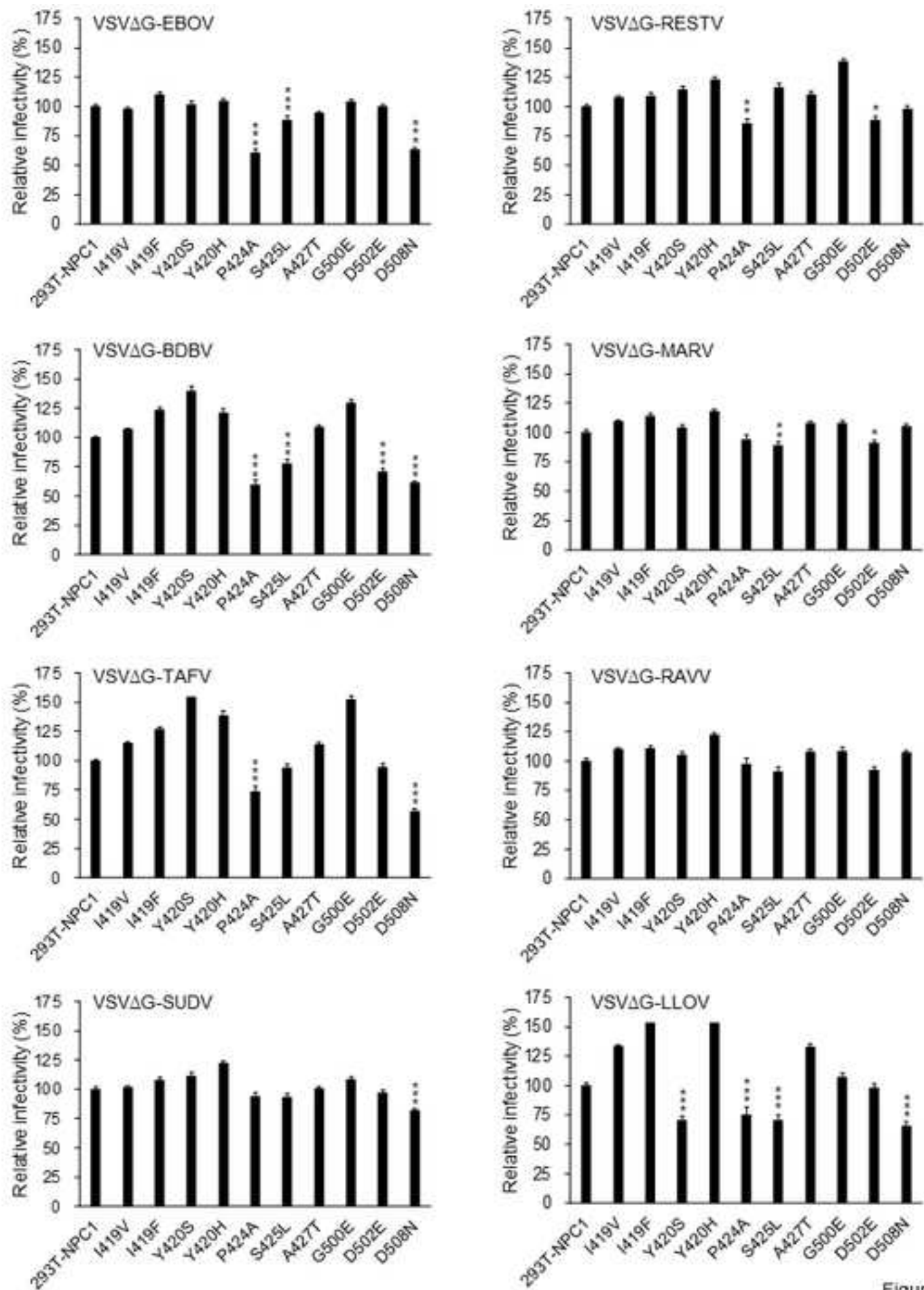


Figure 2

Figure 3

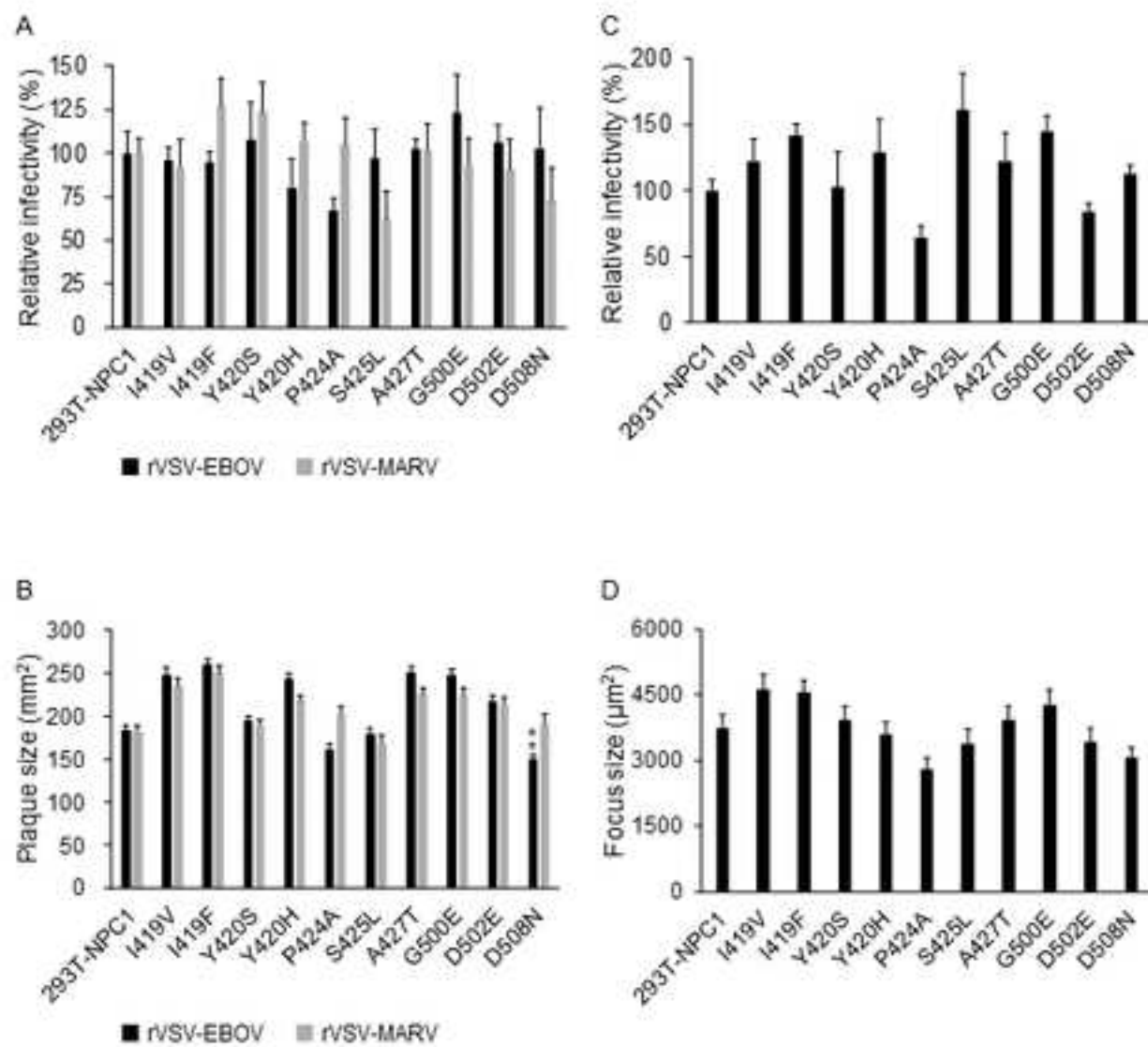


Figure 3